ISSN 0031-918X, Physics of Metals and Metallography, 2018, Vol. 119, No. 3, pp. 216–228. © Pleiades Publishing, Ltd., 2018.
Original Russian Text © L.A. Klinkova, V.I. Nikolaichik, N.V. Barkovskii, V.K. Fedotov, A.F. Shevchun, 2018, published in Fizika Metallov i Metallovedenie, 2018, Vol. 119, No. 3, pp. 232–242.

STRUCTURE, PHASE TRANSFORMATIONS, AND DIFFUSION

The Effect of Synthesis Conditions on the Phase Composition and Structure of $EuBa_2Cu_3O_{6+\delta}$ Samples

L. A. Klinkova[a], *, V. I. Nikolaichik[b], N. V. Barkovskii[a], V. K. Fedotov[a], and A. F. Shevchun[a]

[a] *Institute of Solid State Physics, Russian Academy of Sciences, Chernogolovka, Moscow oblast, 142432 Russia*

[b] *Institute of Microelectronics Technology and High-Purity Materials, Russian Academy of Sciences, Chernogolovka, Moscow oblast, 142432 Russia*

**e-mail: klinkova@issp.ac.ru*

Received February 3, 2017; in final form, September 12, 2017

Abstract—The composition and the structure of ceramic $EuBa_2Cu_3O_{6+\delta}$ (Eu-123) oxide samples annealed in steps with varying processing conditions (in air or oxygen and argon atmosphere at a temperature of 940–960°C for 1–70 h with or without homogenization) were studied by the X-ray phase and chemical analysis, electron diffraction pattern analysis, elemental analysis, and high-resolution transmission electron microscopy. Regardless of the processing conditions, Eu-123 nanostructured oxide with a tetragonal or orthorhombic structure and domains 1–20 nm in size was obtained as a result of annealing. Nanostructuring of the samples, which was revealed by high-resolution electron microscopy, is attributed to their chemical nature: the presence of identical structural elements in members of the homologous $Eu_nBa_mCu_{m+n}O_y$ series of oxides allows them to intergrow coherently and create an illusion of a single crystal. Just like any other member of the $Eu_nBa_mCu_{m+n}O_y$ series, oxide Eu-123 is disproportionate depending on the annealing conditions to form other members of this series located on either side of the dominant oxide. Temperature T_c of the superconducting transition of each member of the series depends on the average oxidation state of copper $\overline{Cu}$. At $\overline{Cu} < 2$, all members of the series have a tetragonal structure and do not exhibit superconducting properties. At $\overline{Cu} = 2.28$, five members of the $Eu_nBa_mCu_{m+n}O_y$ series with matrices (Ba : Cu) 5 : 8, 3 : 5, 2 : 3, 5 : 7, and 3 : 4 exhibit superconducting properties with $T_c = 82–90$ K.

Keywords: $EuBa_2Cu_3O_{6+\delta}$ oxide, $Eu_nBa_mCu_{m+n}O_y$ homologous series, nanostructuring, high-temperature superconductivity

DOI: 10.1134/S0031918X18030067

INTRODUCTION

The study of high-temperature superconducting (HTSC) oxide $EuBa_2Cu_3O_{6+\delta}$ (Eu-123), which is a crystallochemical analog of $YBa_2Cu_3O_{6+\delta}$ (Y-123), provides an opportunity to reveal the effect of the ionic radius of a rare-earth element (0.93 Å for Y^{3+} and 1.03 Å for Eu^{3+}) on structural and superconducting properties. Oxide Y-123 is a nanostructured material containing coherently incorporated inclusions several nanometers in size [1]. The cation composition of these inclusions is established by the existence of the homologous $Y_nBa_mCu_{m+n}O_y$ series [2, 3].

Cation nonstoichiometry of Eu-123 in all three cations was reported in [4]. This nonstoichiometry is established by the existence of a similar $Eu_nBa_mCu_{m+n}O_y$ series [5]. The available literature data on the synthesis conditions and properties of Eu-123 [6–13] are presented in Table 1. It was assumed in [6–11, 13] that Eu-123 has a single-phase and uniform structure. This assumption is based on the results of X-ray diffraction studies. The possibility of variation of the cation composition of Eu-123 (partial substitution of barium for europium) was only noted in [12], although the copper content was still assumed to be constant.

It is well known that Y-123 and Eu-123 with the maximum oxygen saturation ($0.8 < \delta < 1.0$) are formed by twins with a size of 50–100 nm, while the oxides undersaturated with oxygen ($\delta \approx 0.4–0.6$) are composed of domains of oxygen-depleted and oxygen-enriched phases ≈20 nm in size [14–16]. Oxide Y-123 with the maximum oxygen saturation (ortho-phase with a twin structure) and oxide Y-123 undersaturated with oxygen (tetra-phase) are materials with a much finer scale of structural elements (several nanometers). This raises the questions as to whether the structure of Eu-123 depends on the synthesis conditions and how the nanostructure is related to superconducting properties.

Table 1. Literature data on the conditions of synthesizing Eu-123

Initial reagents	Sample composition (Eu : Ba : Cu)	Synthesis conditions				Parameters of the obtained product	Reference
		atm.	T, °C	τ, h	cooling regime		
Eu_2O_3 $BaCO_3$ CuO	123	O_2 O_2 O_2 Air	950 950 → 20 + h.[b] 950 350, 450, 600	50 10 	 s/c[a] N_2 quench N_2 quench	20°C T_c = 90 K, 350°C T_c = 90 K, 450°C T_c = 80 K, 600°C T_c = 50 K (ρ)[c]	[6]
Eu_2O_3 $BaCO_3$ CuO	123	Air O_2 O_2	950 + h. 900 900 → 20	24 12 	 50°C /h	T_c = 91.5 K (χ)	[7]
Eu_2O_3 $BaCO_3$ CuO	123	Air Air O_2 O_2 Air	960 + h. 960 980 980 → 200 200 → 20	10 17 8 	 100°C /h s/c 	T_c = 94.5 K (χ), T_c = 93.7 K (ρ)	[8]
Eu_2O_3 $BaCO_3$ CuO	123	O_2	950 950 → 50 + h. 950 950 → 20	4 15 	 75°C /h 	T_c = 92 K, ΔT_c = 1 K (ρ), T_c = 90 K, ΔT_c = 6 K (χ)	[9]
Eu_2O_3 BaO_2 CuO	123	$0.1O_2$	900 900 → 20 960 960 → 20 (3 h.)	50 50 	 s/c 	δ = 0.38, T_c = 93 K (from 960°C), δ = 0.38, T_c ≈ 45 K (from 900°C) (ρ)	[10]
Eu_2O_3 BaO CuO	123	O_2	960 + 800 with different $P(O_2)$	50 	 	δ = 0.25, T_c = 93 K δ = 0.38, T_c = 60 K δ = 0.5, T_c = 60 K (ρ)	[11]
Eu_2O_3 BaO CuO	$Eu_{1+x}Ba_{2-x}Cu_3O_{7-\delta}$ x = 0.02–0.20	Air O_2	800 950 950 → 500 500 500 → 20	24 25 7 	 s/c 	x = 0, T_c = 93 K x = 0.05, T_c = 91 K x = 0.10, T_c = 83 K x = 0.15, T_c = 67 K x = 0.20, T_c = 55 K (ρ)	[12]
Eu_2O_3 $BaCO_3$ CuO	123	Air O_2	940 + h. 950 400 400 → 20	12 36 24 	 s/c	T_c = 94.5 K (ρ)	[13]

[a] Slow cooling. [b] Samples were homogenized (h.) by grinding and pressing after the specified annealing period. [c] Temperature dependences of either the resistivity (ρ) or the magnetic susceptibility (χ) were used to determine T_c.

In the present study, the effect of the atmosphere, temperature, and duration of the initial annealing, successive annealings, and intermediate homogenization on the phase composition and the structure of Eu-123 samples were examined. The phase composition and the structure of samples were investigated by X-ray phase analysis and elemental analysis (EA) in a transmission electron microscope (TEM) with simultaneous monitoring of electron diffraction (ED) patterns and high-resolution electron microscopy (HREM) data. The average oxidation state of copper $\overline{Cu}$ in the samples was determined by chemical analysis, and the temperature T_c of the superconducting transition was identified by examining the temperature dependence of magnetic susceptibility.

It turned out that nanostructuring is characteristic of Eu-123 and is not affected by the synthesis conditions. However, the composition and the size of inclusions vary depending on the production process and exert a certain influence on the superconducting properties.

Table 2. Conditions of multistage synthesis of Eu-123 samples

Group of samples	Sample no.	Synthesis conditions			Cell parameters of the Eu-123 tetragonal phase			$\overline{Cu}$
		atm.	T, °C	τ, h	a, Å	c, Å	V, Å^3	
1	1-1	Air	940	1	3.879	11.806	177.64	1.79
	1-2	Air	940	6	3.880	11.825	178.01	1.83
	1-3	Ar	940	6h.[a] + 3	3.878	11.827	177.86	1.73
2	2-1	Air	940	1h. + 2	3.880	11.813	177.84	1.78
	2-1	Air	940	1h. + 2h. + 3	3.881	11.814	177.94	1.78
3	3-1	Air	960	19	3.879	11.815	177.78	1.79
	3-2	Air	960	19h. + 28	3.878	11.814	177.67	1.80
	3-3	Air	960	19h. + 28h. + 23	3.879	11.825	177.93	1.79
4	4-1	O_2	950	3h. + 3	3.883	11.786	177.71	1.91
	4-2	O_2	950	3h. + 3h. + 4	3.884	11.792	177.89	1.90

[a] Samples were homogenized (h.) by grinding and pressing after the specified annealing period.

EXPERIMENTAL

Eu_2O_3 (TU 48-4-194-72), BaO_2 (analytical-reagent grade), and CuO (extra-pure grade) were used as the source materials. Oxides were subjected to thermal processing similar to that used in [17]. Stoichiometric mixtures of Eu_2O_3, BaO_2, and CuO were homogenized and pressed into pellets (h = 5 mm, D = 8 mm) in order to synthesize Eu-123. The annealing conditions, which are close to the empirically adjusted conditions detailed in [6–13], are given in Table 2. Pellets were annealed in air, argon, or an oxygen atmosphere ($P(O_2)$ = 101 kPa) in alundum crucibles. Samples were quenched with liquid nitrogen after each stage of annealing; the morphology was not altered by this procedure.

X-ray diffraction (XRD) patterns were measured at room temperature using a Siemens D-500 setup with Cu$K\alpha_1$ radiation and a monochromator. The parameters of unit cells were determined by profile analysis with an error of ±0.005 Å.

Samples for TEM were prepared by cleaving the synthesized crystals (without grinding) in an agate mortar and making a suspension with particles several micrometers in size. The suspension prepared for elemental and diffraction analysis was deposited onto thin carbon films resting on support beryllium grids. These studies were conducted at an accelerating voltage of 100 kV using a JEM-2000FX (JEOL) electron microscope fitted with an INCA elemental energy-dispersive analysis system (Oxford Instruments) and an analytical holder (Gatan) with a beryllium sample cradle. In order to determine the cation composition of oxides, spectra of several dozen particles were measured with simultaneous monitoring of ED patterns. The relative accuracy of determining the cation composition was ±3%.

HREM studies were carried out using a JEM-2100 (JEOL) TEM. Samples for these studies were prepared by depositing the suspension on holey carbon films. The crystal structure was examined at the edges of thin particles within the holes. The substrate did not affect the contrast of electron-microscopy images.

The amount of copper in a formal oxidation state of +3 (Cu(III)/Cu_{tot}, where Cu_{tot} is the total copper content of a sample) was determined by double iodometric titration [18]. The average oxidation state of copper $\overline{Cu}$ was calculated as $\overline{Cu}$ = 2 + Cu(III)/Cu_{tot}. The Cu^+ content (Cu(I)/Cu_{tot}) was determined by dissolving a sample in a hydrochloric Fe(III) salt solution with subsequent titration of the produced Fe(II) by dichromate [19]. The average oxidation state of copper was then calculated as $\overline{Cu}$ = 2 – Cu(I)/Cu_{tot}. Samples were unsealed at argon bubbling of the solutions. The total copper content Cu_{tot} was determined by iodometry. The error in determining $\overline{Cu}$ did not exceed ±0.04.

The measurements of dynamic magnetic susceptibility χ were conducted at a frequency of 100 kHz in the temperature interval of 4–300 K. A sample was placed inside a pair of coaxial coils 6 mm in diameter. One coil produced an alternating magnetic field, and the other one was used for measurements. An identical pair of coils located nearby served to cancel out the signal when a sample was not present. The mismatch signal was measured using the standard synchronous detection scheme. This signal is proportional to magnetic moment $M = \chi VH$, where $H \approx 0.1$ Oe is the strength of the magnetic field produced by the coil, and V is the volume of the sample. Temperature T_c of the onset of the superconducting transition was determined based on the temperature dependence of magnetic susceptibility $\chi = f(T)$ of samples.

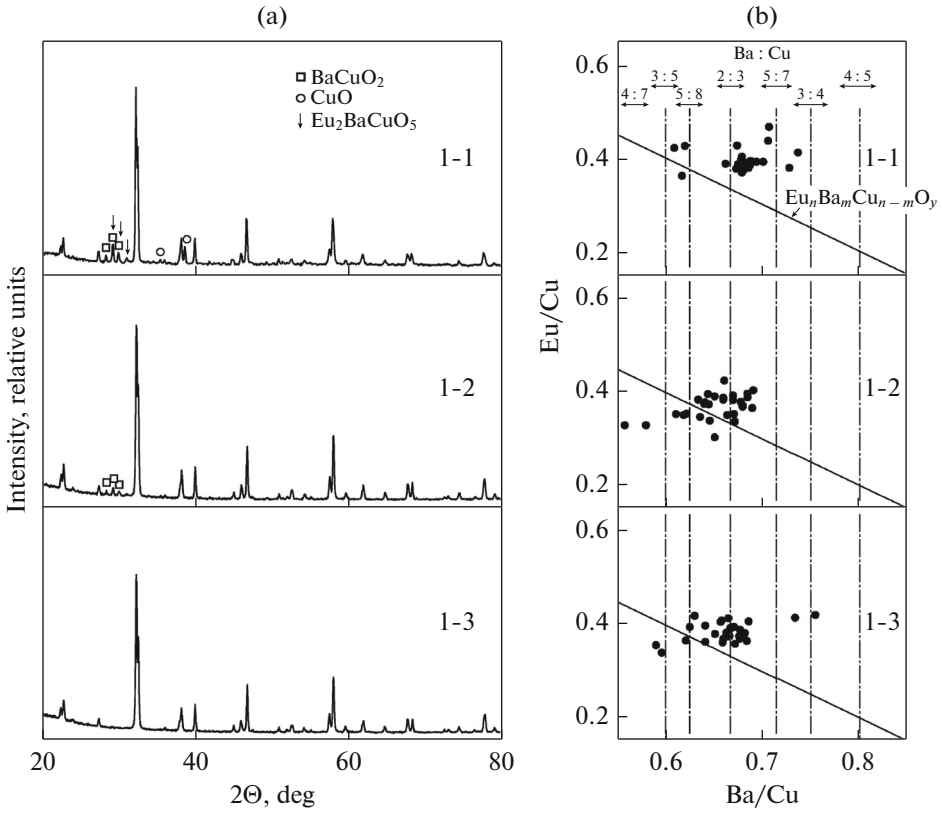

Fig. 1. (a) X-ray diffraction patterns of Eu-123 samples of the first group. Unlabeled peaks correspond to the tetragonal Eu-123 oxide. (b) Cation composition determined based on the EA data for particles of the tetragonal phase.

RESULTS

The samples were divided into four groups with different annealing regimes (Table 2).

Samples of the First Group

Short-term annealing of samples 1-1 and 1-2 for 1 and 6 h at 940°C in air did not result in the synthesis of a single-phase product (Fig. 1), although it facilitated the synthesis of the tetragonal Eu-123 phase. Phases of the Ba–Cu–O ($Ba_mCu_{m+n}O_y$) [20] matrix system with the $BaCuO_2$ structure and a varying composition, Eu_2BaCuO_5, and CuO were present as impurities. Homogenization and subsequent annealing in argon atmosphere (3 h) had a positive effect; the results of an X-ray analysis of sample 1-3 demonstrated that it was single-phase.

The Ba/Cu ratio is plotted on the abscissa in Fig. 1b, vertical lines correspond to oxides $Ba_mCu_{m+n}O_y$, and the Eu/Cu ratio is plotted on the vertical axis. The sloping straight line corresponds to the stoichiometric compositions of members of the $Eu_nBa_mCu_{m+n}O_y$ homologous series [5]. According to the EA data, the samples of the first group are characterized by a nonuniform cation composition in the range of matrix oxides (Ba : Cu) (3 : 5)–(3 : 4).

Samples of the Second Group

Sample 2-1 differed from sample 1-1 in that it was subjected to homogenization after annealing for 1 h at 940°C (Fig. 2a). At this stage, its X-ray pattern corresponded to single-phase tetragonal Eu-123. Additional homogenization and subsequent annealing for 3 h in the same regime did not alter its nature (sample 2-2). The parameters of the tetragonal phase of samples 2-1 and 2-2 (Table 2) and the $\overline{Cu}$ values in these samples were close. This suggests that the short-term annealing of the initial oxide mixture at 940°C for 1 h with subsequent homogenization and additional annealing in the same regime are sufficient to produce an X-ray single-phase sample. The EA data (Fig. 2b) showed that the cation composition of the studied particles of samples 2-1 and 2-2 differed considerably from the nominal 123 composition. However, their XRD pattern was that of a single-phase sample.

Samples of the Third Group

Long-term annealing of the samples of the third group in air at 960°C with homogenization after each annealing stage did not result in the complete removal of impurity phases $BaCuO_2$ and Eu_2BaCuO_5, but their fraction decreased gradually, while the fraction of

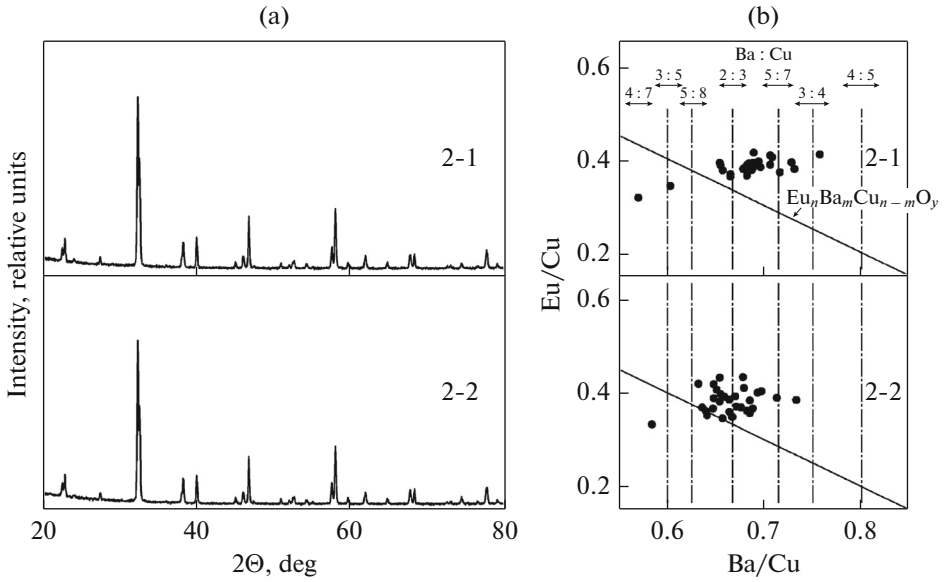

Fig. 2. (a) X-ray diffraction patterns of Eu-123 samples of the second group. (b) Cation composition determined based on the EA data for particles of the tetragonal phase.

Eu-123 increased to 97.8 wt % after 70 h of annealing (Fig. 3a). The cation composition of particles of the tetragonal Eu-123 phase varied in the process of annealing; it shifted gradually toward the composition of barium-rich matrix oxides starting from the dominant oxides with matrices 4 : 7 and 3 : 5 in sample 3-1 (Fig. 3b).

Samples of the Fourth Group

The fourth group of samples were annealed in oxygen atmosphere at 950°C for 6 and 10 h with intermediate homogenization. At the end of the first annealing stage, sample 4-1 contained $BaCuO_2$; in the process of further annealing, the fraction of this impurity phase was reduced to trace levels (Fig. 4a). According to the results of EA of particles of the tetragonal Eu-123 phase in samples 4-1 and 4-2, their cation composition differed from the stoichiometric composition at all stages of annealing (Fig. 4b). Particles with matrices (Ba : Cu) 2 : 3 and 5 : 7 were dominant. Oxides with matrix 3 : 5 were lacking. Almost all particles were enriched with europium in excess of stoichiometry. The samples were enriched in oxygen ($\overline{Cu}$ = 1.90–1.91). The tetragonal cell parameters were close to the reference values for $EuBa_2Cu_3^{+1.75}O_{6.13}$: a = 3.879(1) Å, c = 11.811(1) Å, and V = 177.72 Å^3 [21] (Table 2).

Annealing of Samples in Oxygen Atmosphere at 450°C for 5 h

The Eu-123 phase in samples of all four groups acquired an orthorhombic structure after oxygen annealing (Fig. 5a). However, the cation composition of particles with this structure remained inhomogeneous (Fig. 5b). The XRD patterns did not reveal this inhomogeneity; according to the XRD data, samples 1-4, 2-3, 4-3, and 4-4 were single-phased. The parameters of the orthorhombic Eu-123 phase (Table 3) differed somewhat from those determined for $EuBa_2Cu_3O_7$ ($\overline{Cu}$ = 2.33) (a = 3.8973 Å, b = 3.8384 Å, c = 11.7069 Å,

Table 3. Parameters of the orthorhombic cell of Eu-123

Sample no.	Cell parameters				$\overline{Cu}$
	a, Å	b, Å	c, Å	V, Å^3	
1-4	3.905	3.844	11.711	175.79	2.28
2-3	3.904	3.844	11.705	175.66	2.24
3-4	3.905	3.841	11.705	175.56	2.28
4-3	3.903	3.850	11.708	175.93	2.29
4-4[a]	3.900	3.851	11.694	175.63	2.28

[a] The sample was cooled slowly (50°/h) to 20°C.

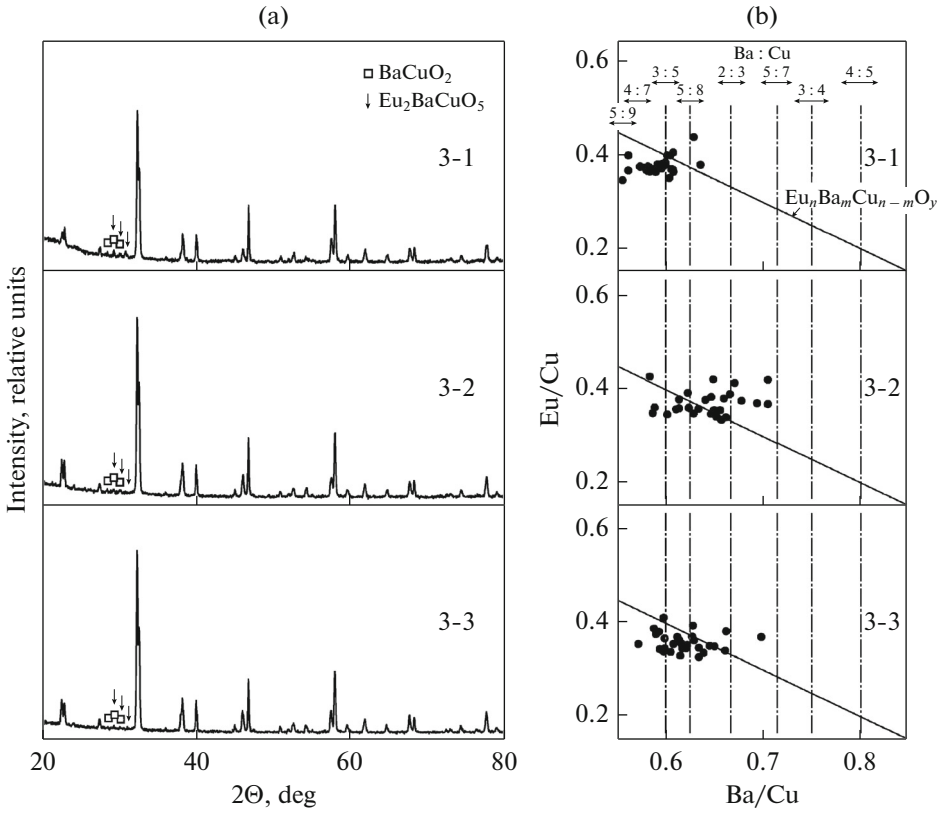

Fig. 3. (a) X-ray diffraction patterns of Eu-123 samples of the third group. (b) Cation composition determined based on EA data for particles of tetragonal phase.

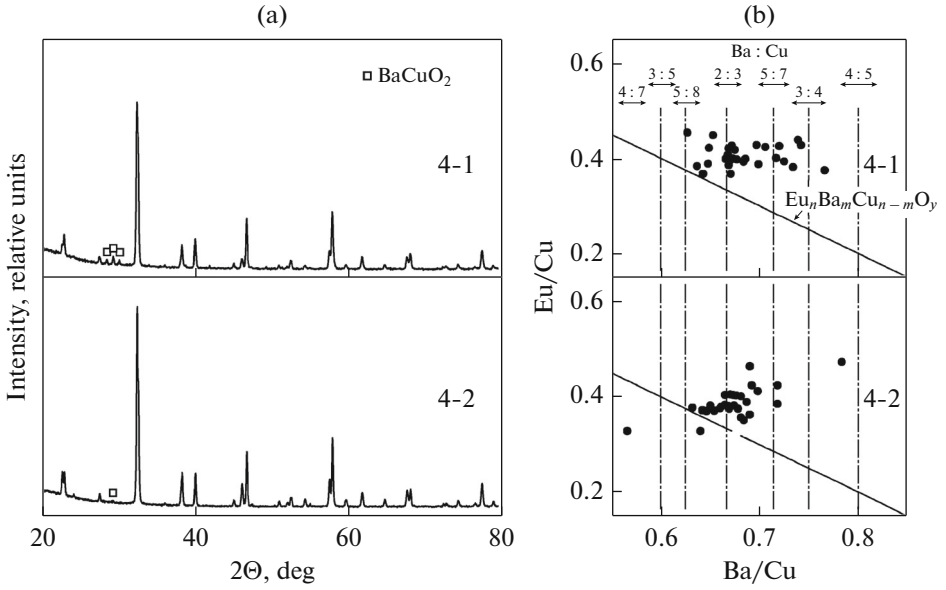

Fig. 4. (a) X-ray diffraction patterns of Eu-123 samples of fourth group. (b) Cation composition determined based on EA data for particles of tetragonal phase.

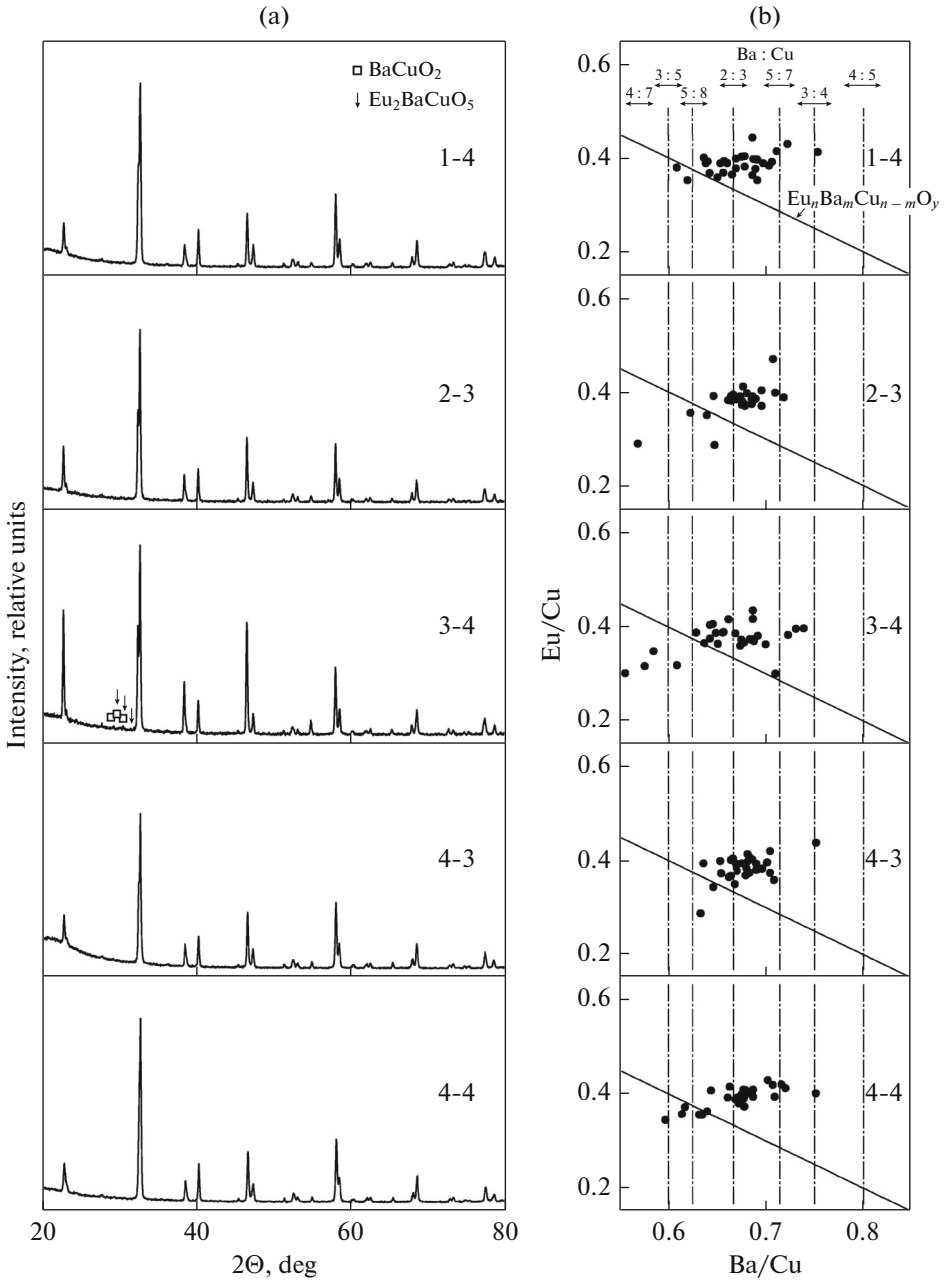

Fig. 5. (a) X-ray diffraction patterns of Eu-123 samples of all four groups after oxygen annealing at 450°C (5 h). (b) Cation composition determined based on the EA data for particles of the orthorhombic phase. Sample 4-4 was cooled slowly (50 K/h) to 20°C.

and $V = 175.13$ Å^3) [22]. This may be attributed to the difference in the $\overline{\text{Cu}}$ values.

Superconducting Properties of Samples with the Orthorhombic Phase

Sample 1-4 had a narrow superconducting transition starting at 88 K in the $\chi = f(T)$ dependence (Fig. 6a). The bends at 86, 85, and 82 K indicate the presence of several superconducting phases in sample 1-4. The phase with $T_c = 82$ K produced the dominant contribution. The $\chi = f(T)$ dependence for sample 2-3 revealed an extended superconducting transition starting at $T_c = 86$ K and ending at 20 K (Fig. 6a). Thus, the introduction of two additional homogenizations had no positive effect on the T_c value of the orthorhombic Eu-123 phase.

The three-phase composition of sample 3-3 (Fig. 3b) was retained after additional annealing in oxygen at 450°C for 5 h (sample 3-4, Fig. 5b). The composition range of particles of the orthorhombic Eu-123 phase in sample 3-4 was the widest at (5 : 9)–

(3 : 4). The magnetic susceptibility curve of this multiphase system (Fig. 6b) had bends corresponding to superconducting phases with T_c = 88, 86, 85, and 82 K. In contrast to sample 1-4, the phases in sample 3-4 produced comparable contributions. Thus, longer (70 h) annealing at a higher temperature (960°C) with homogenization performed after each annealing stage facilitated the formation of phases with high T_c values (82–88 K).

Samples 4-1 and 4-2 did not exhibit superconducting properties ($\overline{Cu}$ = 1.91 and 1.90, respectively). Samples 4-3 and 4-4 were superconducting (Fig. 6c), but had considerably different properties. Sample 4-3 ($\overline{Cu}$ = 2.29), which was quenched from 450°C, had T_c = 78 K, while the superconducting transition in sample 4-4 ($\overline{Cu}$ = 2.28), which was slowly (50°/h) cooled in oxygen to 20°C, was initiated at 90 K, and dependence $\chi = f(T)$ had bends in the range of 82–90 K and was similar in shape to the dependence for sample 1-4. Thus, the use of an oxygen atmosphere in the synthesis of rhombic Eu-123 did not offer any noticeable advantages over annealing in air with additional processing in oxygen atmosphere at 450°C.

Samples 4-4 and 4-3 had close $\overline{Cu}$ values (2.28 and 2.29, respectively). These samples were also similar in terms of their cation composition and differed only in that the oxide with matrix 3 : 5 was present in sample 4-4. Therefore, sample 4-3 with T_c = 78 K should be considered oversaturated with oxygen ($\overline{Cu}$ = 2.29). This oversaturation resulted in the loss of superconducting properties of certain phases with T_c = 82–90 K.

HREM Studies of the Nanostructure of Eu-123 Samples

HREM images of particles of all the studied oxides revealed nonuniform structures with two types of nonuniformities. Nonuniformities of the first type manifested as darker or lighter (compared to the surrounding areas) regions with a size of just one or several nanometers seen in the image taken in the [001] direction (Fig. 7a). When viewed along the [100] direction (Fig. 7b), these regions appear as dark stripes parallel to planes (001). The crystal regions corresponding to these dark stripes had a thickness of 2–3 interplanar distances d_{006}. The distance between these regions measured along planes (001) did not exceed 5 nm. Evidently, their crystal structure differed from that of the surrounding areas.

Nanostructural nonuniformities of the second type manifested as regions 10–20 nm in size with a blurred image of the crystal lattice. More often than not, the intensity of these regions of HREM images also differed from the intensity averaged over the sample (Figs. 7a, 8a). The aforementioned blurriness can be attributed to the local lattice misalignment with the incident electron beam (lattice directions [001] or [100] in regions with a clear image of the atomic structure are perfectly aligned with the incident beam).

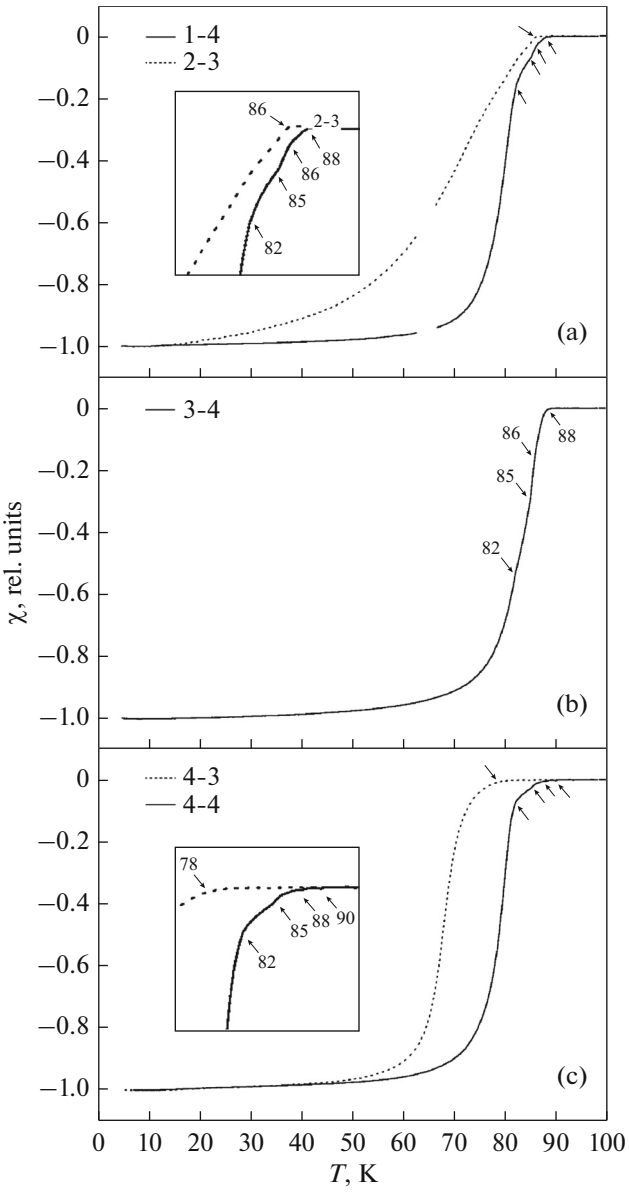

Fig. 6. Temperature dependences of magnetic susceptibility $\chi = f(T)$ of samples (a) 1-4 and 2-3, (b) 3-4, and (c) 4-3 and 4-4.

The examination of ED patterns and HREM images of samples revealed their qualitative similarity. The ED patterns (insets in Figs. 7 and 8) did not have any signs of nonuniformity or defects (strands, diffuse scattering). This suggests that both types of heterogeneous regions had close crystal structures and were matched coherently to the structure of the primary phase.

The presence of nonuniformities with typical sizes of 10–30 nm in an Nd-123 superconductor, which is

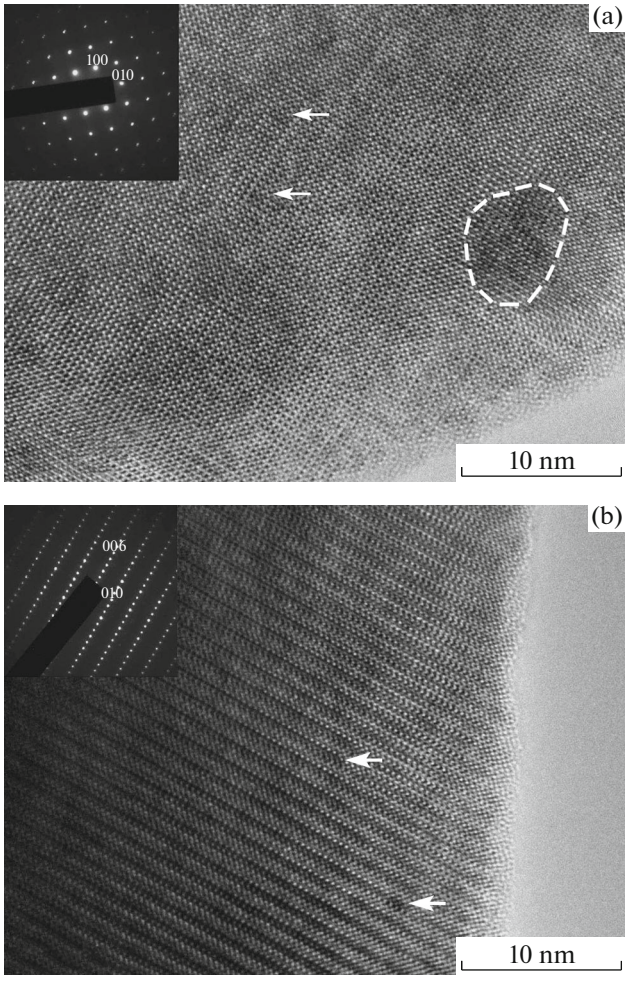

Fig. 7. HREM images and ED patterns (insets) of particles of sample 2-3 along directions (a) [001] and (b) [100]. Nanoirregularity regions of the first type are indicated by arrows, and second-type irregularities are indicated by dashed lines.

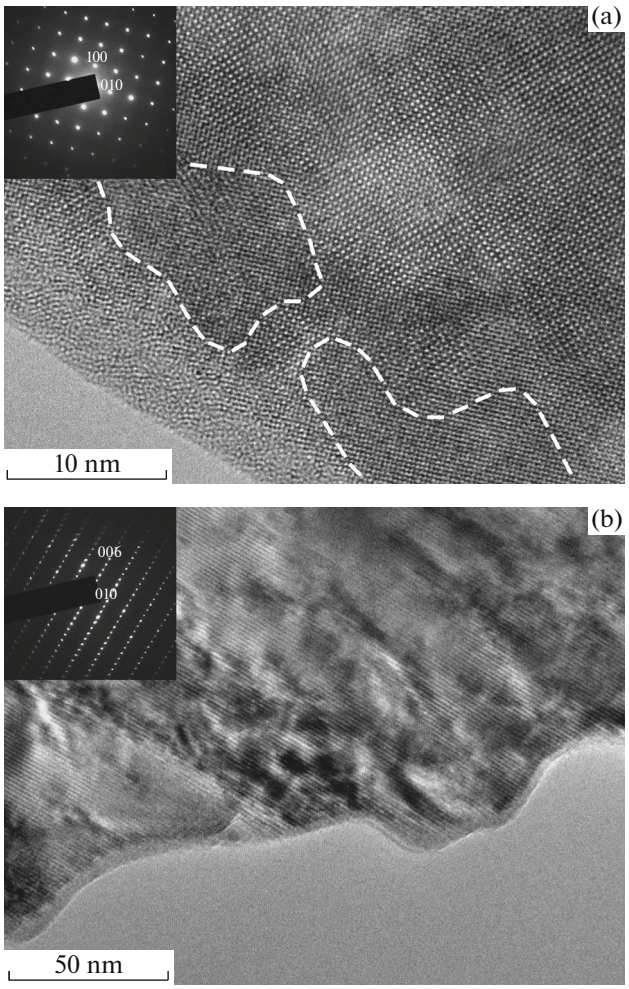

Fig. 8. HREM images and ED patterns (insets) of particles of sample 3-4 along directions (a) [001] and (b) [100]. Nanoirregularity regions of the second type are outlined with dashed lines.

an analog of Eu-123, was noted in [23–25]. These nonuniformities were attributed to the local nonstoichiometry of the cation [25]. Thus, the obtained data regarding the presence of nonuniformities of the second type with a typical size of 10–20 nm in Eu-123 agree with the literature data [23–25] and substantiate the assumption that these nonuniformities are associated with the local cation nonstoichiometry. The observation of nonuniformities of the first type with a typical size of several nanometers is an essential addition to the already available data. These features were not observed in [23–25], since the images obtained in these studies did not have the required atomic-level resolution.

It was assumed in [26] that the inhomogeneous state of RE-123 superconductors with light REs (rare-earth elements) is established by spinodal decomposition, which produces enriched and depleted regions with different RE/Ba ratios. The authors of [26] believed that the ordered state of RE and Ba atoms could be present in enriched and depleted regions; this is assumed in the present study. The obtained data suggest that the RE/Ba ratio varies discretely in these regions.

Hypothetical structure cells (cation sublattice) of members of the $Eu_nBa_mCu_{m+n}O_y$ homologous series (123, 235, and 257) are shown in Fig. 9. The presence of identical structural units in cells allows the crystal domains of members of this series to intergrow coherently and form a pseudosingle crystal with an averaged structure of the Eu-123 phase.

Contribution of Nonstoichiometric Europium to the Structuring of Oxides of the $Eu_nBa_mCu_{m+n}O_y$ Series

The question then arises as to what positions in domains of oxides of the $Eu_nBa_mCu_{m+n}O_y$ series are

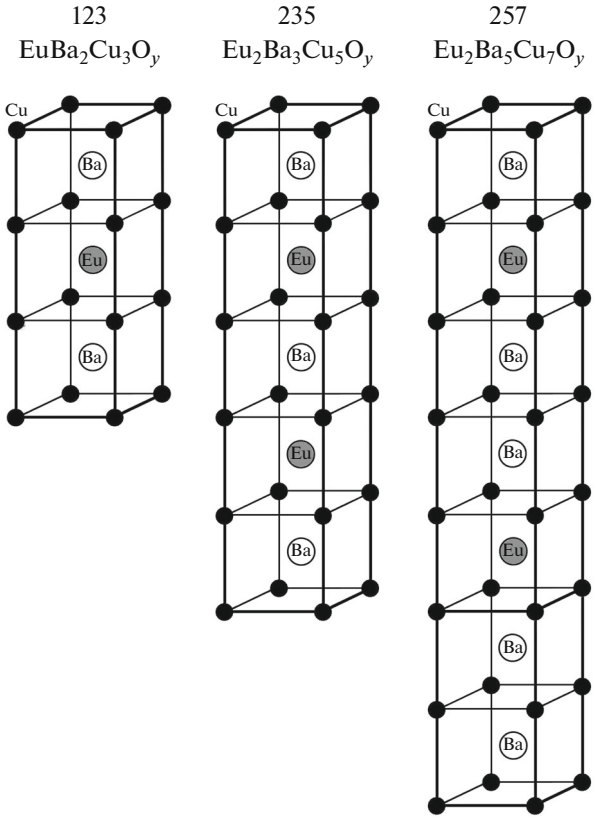

Fig. 9. Hypothetic structure of the cation sublattice of members of the $Eu_nBa_mCu_{m+n}O_y$ homologous series with the following compositions (Eu : Ba : Cu): 123, 235, and 257.

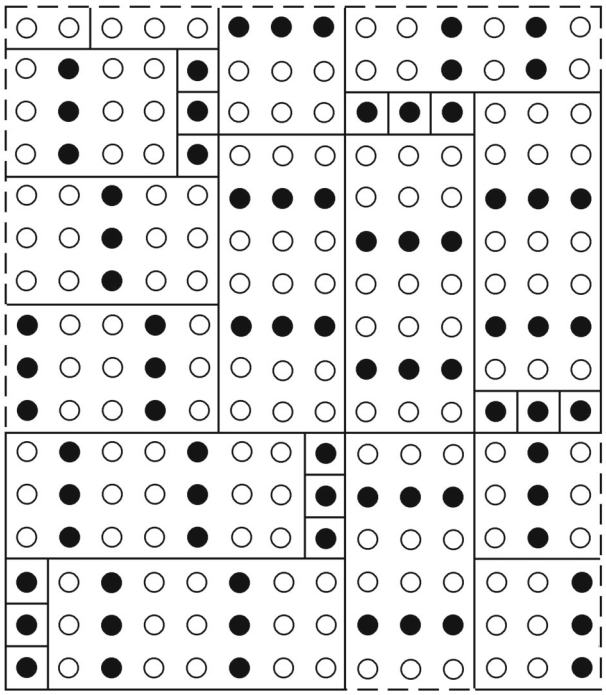

Fig. 10. Irregular arrangement of units of three Eu-257 oxide cells (open and filled circles denote barium and europium) and excess europium (squares with filled circles).

occupied by excess europium revealed by EA. Excess europium can occupy irregular positions in domains of oxides of the $Eu_nBa_mCu_{m+n}O_y$ series and, thus, form no superlattice structure. Figure 10 shows a hypothetical diagram for Eu-123, where a coherent intercell of three europium atoms is formed in the unit system of three 257 cells and three excess europium ions. In $Eu_{2.33}Ba_5Cu_7O_y$, one europium atom is added to three $Eu_2Ba_5Cu_7O_y$ cells.

Samples 1-4 and 3-4 contain 0.6 atoms of excess europium per a particle of the $Eu_{2.6}Ba_5Cu_7O_y$ composition (three europium atoms per five 257 cells). The estimated europium excess is ~30%.

The second question concerns the source of this excess europium. The material balance of Eu, Ba, and Cu atoms should be maintained in the synthesized samples; it is maintained if the impurity phases are factored in. In some samples, these impurity phases ($BaCuO_2$, CuO, Eu_2BaCuO_5) with a composition differing greatly from Eu-123, were detected by X-ray analysis; in other samples, TEM studies that reveal individual particles of impurity phases were required.

The next question concerns the fraction of europium in each particle, which establishes the necessary Eu-123 structure. The compositions in Fig. 5b provide an answer to this question. The excess europium in particles with matrices 3 : 5 and 5 : 8 may be as large as 10 and 17%, while the europium deficiency can be as large as 20 and 7%, respectively. The europium excess in particles with matrices 2 : 3 and 5 : 7 can be as significant as 29 and 48%, respectively.

DISCUSSION

Effect of Temperature on the Process of Synthesis of Eu-123

The temperature of the first stage of annealing of sample 3-1 (960°C) was somewhat higher than that of sample 1-1. This facilitated the synthesis of copper-rich oxides with matrices (Ba : Cu) 5 : 9, 4 : 7, 3 : 5, and 5 : 8. While the annealing time of sample 3-1 was also increased to 19 h, this does not alter the conclusion above, since subsequent annealings of this sample with intermediate homogenizations were not conducive to preservation of its initial cation composition. The sample composition changed in the process of homogenization and subsequent annealing; oxides formed at the first stage of annealing were partially preserved.

When the temperature of the first stage of annealing was raised from 940 to 960°C, the fraction of the $BaCuO_2$ impurity phase, which did not disappear in

the process of further annealing, increased. This is attributed to the fact that, under these conditions, no barium-rich oxide with matrix 3:4 was formed. The synthesis of this oxide was initiated in the process of additional oxygen annealing (450°C, 5 h), which facilitated the decomposition of oxides with matrices 5 : 9, 4 : 7, and 3 : 5 (sample 3-4). This sample had the highest fraction of phases with T_c = 82–88 K and the widest range of variation in the cation composition of the Eu-123 phase (Ba/Cu = 0.55–0.75). For comparison, Ba/Cu = 0.60–0.75 in sample 1-4.

Effect of Homogenization in the Synthesis of Eu-123 Oxide

The results of comparison of superconducting properties of samples 1-4 ($\overline{Cu}$ = 2.28, T_c = 82–88 K) and 2-3 ($\overline{Cu}$ = 2.24, T_c = 20–86 K), which were first annealed at 940°C, suggest that double homogenization had a negative effect on samples. The conditions of oxygen annealing were the same (450°C, 5 h), but sample 2-3 had less oxygen. This is why the oxides present in this sample were undersaturated with oxygen and europium. It is quite likely that the reason why these oxides have lower T_c values (despite that the cation compositions of matrices are centered around oxide 2 : 3) is the same.

However, initial annealing with double homogenization in air at 960°C and long-term holding (sample 3-4) did not adversely affect the superconducting properties of this sample emerging after its additional oxygen annealing.

Effect of Annealing Duration on the Superconducting Properties of Eu-123 Oxide Samples

The effect of the duration of annealing is identified based on the variations in the parameters of samples from the third group with the finest superconducting properties. It can be seen that the faction of impurity oxides $BaCuO_2$ and Eu_2BaCuO_5 decreased as the annealing time increased from 19 to 47 h. However, the values of $\overline{Cu}$ = 1.79–1.80, which agree within the limits of method error, in samples with the tetragonal phase were not affected by a further increase in annealing time (to 70 h). No clear pattern of variations in the parameters of tetragonal and orthorhombic phases with annealing time could be traced.

Effect of Oxygen Atmosphere at the First Stage of Annealing of Eu-123 Oxide Samples

The product synthesized at the first stage of annealing of sample 4-1 in oxygen atmosphere at 950°C with two homogenizations was not single-phased and contained $BaCuO_2$ impurities. The average copper oxidation state was 1.91 (sample 4-1) or 1.90 (sample 4-2). The oxides assumed a tetragonal structure with cell parameters falling between those of tetragonal and orthorhombic phases (Table 2). Samples 4-1, 4-2, and 4-3 differed from the first three groups of samples in that they lacked oxides with copper-rich matrices (Ba : Cu = 3 : 5). These oxides formed in sample 4-4 during slow cooling in an oxygen atmosphere to room temperature. This is likely attributable to the disproportionation of matrices (e.g., 4(2 : 3) → 3 : 5 + 5 : 7). The coexistence of these matrix oxides has already been reported [20]. The superconducting transition in sample 4-4 ($\overline{Cu}$ = 2.28), which was obtained by cooling sample 4-2 slowly from 950°C to 450°C, annealing at this temperature for 5 h, and then cooling slowly to 20°C, was observed at 90 K. Three bends at 88, 85, and 82 K can be seen in the $\chi = f(T)$ dependence.

Sample 4-3 quenched from 450°C after 5 h of annealing differed from samples 2-3 and 1-4 in that it had a much lower temperature of the onset of the superconducting transition (78 K) and a higher $\overline{Cu}$ value (2.29). However, with the partial change in the cation composition in the orthorhombic phase taken into account, sample 4-3 can be considered to have the same cation composition as the preceding samples, but is overdoped with oxygen. This overdoping may result in the suppression of superconducting properties of oxides, i.e., the reduction of T_c from 82–90 to 78 K.

The obtained data suggest that it is undesirable to introduce the initial annealing of Eu-123 samples in the oxygen atmosphere into the synthesis process.

Thus, the examination of microstructures of Eu-123 samples and the joint analysis of structural data, the cation composition, and the data on superconducting properties reveal the relations between these parameters and provide an opportunity to characterize the effect of synthesis conditions on the superconducting properties of samples. These relations stem from the chemical nature of Eu-123 samples, which is governed by oxides of the $Eu_nBa_mCu_{m+n}O_y$ series that form in the melt through intercalation [5] and inherit the structure of matrix oxides $Ba_mCu_{m+n}O_y$ [20].

CONCLUSIONS

(1) Eu-123 samples were annealed for 1–70 h at temperatures in the range of 940–960°C in air, oxygen, or an argon atmosphere with or without intermediate homogenization. Regardless of the processing conditions, nanostructured objects with the structure of a tetragonal or orthorhombic Eu-123 oxide phase and domains 1–20 nm in size were obtained.

(2) The nanostructuring of these objects is attributed to their chemical nature; the presence of identical structural elements in oxides of the homologous $Eu_nBa_mCu_{m+n}O_y$ series allows them to intergrow coherently and create an illusion of a pseudo-single crystal.

(3) Just as any other member of the $Eu_nBa_mCu_{m+n}O_y$ series, oxide Eu-123 is disproportionate depending on the annealing conditions to form other members of this series located on either side of the dominant oxide.

(4) Members of the $Eu_nBa_mCu_{m+n}O_y$ series undergo a transition from the tetragonal phase to the orthorhombic one and acquire superconducting properties in the process of the additional annealing in oxygen atmosphere. Temperature T_c varies from one member of the series to another.

(5) The T_c value of each member of the series depends on the average oxidation state of copper $\overline{Cu}$. At $\overline{Cu} < 2$, all members of the series have tetragonal structures and do not exhibit superconducting properties. At $\overline{Cu} = 2.28$, five members of the $Eu_nBa_mCu_{m+n}O_y$ series with matrices (Ba : Cu) 5 : 8, 3 : 5, 2 : 3, 5 : 7, and 3 : 4 exhibit superconducting properties with $T_c = 82$–90 K.

(6) Eu-123 samples differ from Y-123 in that they have larger inclusions of the second type. This can be attributed to the fact that Eu^{3+} has a larger ionic radius than Y^{3+}. The trend becomes more evident in Nd-123 [23–25], where even micrometer-sized inclusions can be observed.

ACKNOWLEDGMENTS

This study was supported financially in part by the program Current Problems of Low-Temperature Physics of the Presidium of the Russian Academy of Sciences.

REFERENCES

1. L. A. Klinkova and V. I. Nikolaichik, "Nanostructural inhomogeneity of $YBa_2Cu_3O_{7-\delta}$," Physica C **506**, 33–39.
2. L. A. Klinkova, V. I. Nikolaichik, N. V. Barkovskii, A. F. Shevchun, and V. K. Fedotov, "Existence of the homologous series of $Y_nBa_mCu_{m+n}O_y$ ($m = 2, 3, 5$; $n = 1, 2$) oxides with the tetragonal and orthorhombic structures of $YBa_2Cu_3O_{6+\delta}$," Russ. J. Inorg. Chem. **57**, 1196–1209 (2012).
3. L. A. Klinkova, V. I. Nikolaichik, Q. M. Ramasse, and P. Abellan, "Local variations of cation composition on a nanometer-sized scale in a $YBa_2Cu_3O_{6.92}$ superconductor," J. Supercond. Novel Magn. **29**, 1139–1143 (2016).
4. V. I. Nikolaichik and L. A. Klinkova, "Nanostructural Inhomogeneity of $EuBa_2Cu_3O_{6+\delta}$ Superconductors," Bull. Russ. Acad. Sci.: Fiz. **80**, 1418–1420 (2016).
5. L. A. Klinkova, V. I. Nikolaichik, N. V. Barkovskii, and V. K. Fedotov, "Primary crystallization field of the oxide $EuBa_2Cu_3O_{6+\delta}$ and the existence of a homologous series $Eu_nBa_mCu_{m+n}O_y$ ($m = 2, 3, 4, 5$; $n = 1, 2$)," Russ. J. Inorg. Chem. **60**, 276–284 (2015).
6. T. Iwata, M. Hikita, Y. Tajima, and S. Tsurumi, "Study of the crystal structure of the high temperature superconductor $Eu_1Ba_2Cu_3O_{7-y}$," J. Cryst. Growth **85**, 661–664 (1987).
7. S. A. Hodorowicz, W. Lasocha, A. Lasocha, and H. A. Eick, "The preparation and magnetic behavior of $EuBa_2Cu_{3-y}M_yO_{6.5+x}$ (M = Ni, Co, Al, and Zn) and some related compounds," J. Solid State Chem. **77**, 148–155 (1988).
8. G. Bednorz, G. Stroink, and M.-A. White, "A Study of the heat capacity of the superconductor $EuBa_2Cu_3O_{7-x}$," Physica C **165**, 385–390 (1990).
9. A. V. Dubovitskii, N. V. Kireev, N. D. Kushch, E. F. Makarov, M. K. Makova, A. T. Mailybaev, V. A. Merzhanov, S. I. Pesotskii, R. A. Stukan, and D. M. Shashkin, "Chemivam modification of the high-temperature superconductor $Eu_1Ba_2Cu_3O_{7-\delta}$ with tin: Synthesis, structure, electrophysical properties, and Mössbauer studies," Sverkhprovod.: Fiz., Khim., Tekh. **3**, 1092–1103 (1990).
10. L. Malavasi, A. Tamburini, P. Galinetto, P. Ghigna, and Gl. Flor, "The high-temperature superconductor $EuBa_2Cu_3O_{6+x}$: Role of thermal history on microstructure and superconducting properties," J. Mater. Synthes. Processing **9**, 31–37 (2001).
11. E. Annese, G. Allodi, R. De Renzi, L. Malavasi, and P. Ghigna, "Phase Separation in Superconducting $EuBa_2Cu_3O_{6+x}$," Physica B **326**, 321–324.
12. Y. Li, Y. Liu, R. Duan, X. Xiong, B. Wang, G. Cao, L. Wei, D. N. Zheng, Z. X. Zhao, and J. H. Ross, "Positron annihilation study of the O-T phase transition for $Eu_{1+x}Ba_{2-x}Cu_3O_{7-\delta}$ superconductors," Physica C **402**, 179–187.
13. Z. Chen, J. Zhang, Y. Su, Y. Xue, and G. Cao, "Effect of rare-earth ion size on local electron structure in $RBa_2Cu_3O_{7-\delta}$ (R = Tm, Dy, Gd, Eu, Nd and Y) superconductors: A positron study," Physica C **434**, 161–166.
14. E. I. Kuznetsova, Yu. V. Blinova, S. V. Sudareva, I. B. Bobylev, E. P. Romanov, and T. P. Krinitsina, "X-ray Diffraction Study of Spinodal Decomposition of a Nonstoichiometric Y–Ba–Cu–O Compound," Phys. Met. Metallogr. **95**, 65–70 (2003).
15. S. V. Sudareva, E. P. Romanov, T. P. Krinitsina, Yu. V. Blinova, and E. I. Kuznetsova, "Mechanism of Phase Transformations and Fine Structure of a Nonstoichiometric Compound $YBa_2Cu_3O_{7-\delta}$ at Temperatures of 200 and 300°C," Phys. Met. Metallogr. **102** (2), 205–212 (2006).
16. E. P. Romanov, S. V. Sudareva, E. N. Popova, and T. P. Krinitsina, *Low-Temperatureand High-Tempera-*

ture Suprconductors and Related Composites (UrO RAN, Ekaterinburg, 2009) [in Russian].

17. L. A. Klinkova, N. V. Barkovskii, S. S. Khasanov, and K. V. Van, "Study of the behavior of of the cuprates $Ba_2Cu_3O_y$ and $YBa_2Cu_3O_y$ in molten KOH," Sverkhprovod.: Fiz., Khim., Tekh. **7**, 377–384 (1994).
18. D. C. Harris and T. A. Hewston, "Determination of Cu^{3+}/Cu^{2+} ratio in the superconductor $YBa_2Cu_3O_{8-x}$," J. Solid State Chem. **69**, 182–185 (1987).
19. Y. Saito, T. Noji, K. Hirokawa, A. Endo, N. Matsuzaki, M. Katsumata, and N. Higuchi, "Determination of valence of copper and oxygen deficiency in superconducting $Sr_xLa_{2-x}CuO_{4-y}$," Jpn. J. Appl. Phys. **26**, L838–L839 (1987).
20. L. A. Klinkova, V. I. Nikolaichik, N. V. Barkovskii, and V. K. Fedotov, "On the existence of a homologous series of $Ba_mCu_{m+n}O_y$ oxides with the cubic structure of the $BaCuO_2$ oxide," Physica C **470**, 2067–2071 (2010).
21. ICSD No. 78467.
22. ICSD No. 65392.
23. M. Murakami, N. Sakai, T. Higuchi, and S. I. Yoo, "Melt-processed light rare earth element–Ba–Cu–O," Supercond. Sci. Technol. **9**, 1015–1032 (1996).
24. T. Egi, J. G. Wen, K. Kuroda, H. Unoki, and N. Koshizuka, "High critical-current density of $Nd(Ba,Nd)_2Cu_3O_{7-\delta}$ single crystals," Appl. Phys. Lett. **67**, 2406–2408 (1995).
25. W. Ting, T. Egi, R. Itti, K. Kuroda, N. Koshizuka, S. Tanaka, "Surface electronic properties and atomic images of the as-prepared $Nd_1Ba_2Cu_3O_y$ single crystals," Jpn. J. Appl. Phys. **35**, 4034–4037 (1996).
26. Yu. D. Tret'yakov and E. A. Gudilin, "Chemical principles of the preparation of metal-oxide superconductors," Usp. Khim. **69**, 3–40 (2000).

Translated by D. Safin